Solid-State Electronics 186 (2021) 108140

Contents lists available at ScienceDirect

Solid State Electronics

journal homepage: www.elsevier.com/locate/sse

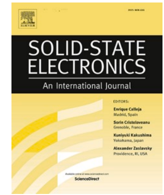

The observation window and the statistical modeling of RTN in time and frequency domain

Gilson Wirth

Electrical Eng. Dept.UFRGS – Unv. Federal do Rio Grande do Sul Porto Alegre, Brazil

ARTICLE INFO

The review of this paper was arranged by "S. Cristoloveanu"

Keywords:
Low-frequency noise
Random telegraph noise (RTN)
Charge trapping
Time dependent variability
Jitter

ABSTRACT

Charge trapping is studied in the context of random telegraph noise (RTN) and low-frequency noise ($1/f$ noise), aiming unified statistical modeling. Analytical formulations for $1/f$ noise (frequency domain) and RTN (time domain) have been derived, using a single modeling framework, where model parameters are the same in frequency and time domain. The modeling addresses the time dependent variability in the electrical behavior of MOSFETs, discussing the variability due to a single trap and the ensemble of traps. In the work here presented we detail the role of the observation window, in both time and frequency domain. We discuss how it impacts the variance of drain current (or threshold voltage) measured over time, and the number of observable traps in a given time window or frequency window. Besides analytical modeling, experimental results are presented and discussed.

1. Introduction

In MOSFETs, the capture and emission of charge carriers by electrically active defects (charge traps) produces fluctuations of the drain current I_D, which may, likewise, be observed as fluctuations of the threshold voltage V_T [1–14]. In time domain, these switching events cause I_D (or V_T) to vary randomly over time, leading to a statistical variance in the observed I_D, as seen in Fig. 1. This randomly varying I_D – or a randomly varying V_T, may cause jitter of signals (time dependent variability). In frequency domain, the spectral density of a single trap has a Lorentzian-like spectrum. The superposition of multiple Lorentzians yields the $1/f$ noise [1,2,7]. Similarly, in time domain, the collective contribution of multiple traps leads to a logarithmic increase of I_D variance with time window, as shown in section II below.

To statistically model the RTN fluctuations following assumptions are done [1–4]: *i)* Charge trapping and de-trapping are stochastic events governed by characteristic time constants. The characteristic time constant of a trap is a random variable assumed to be uniformly distributed on a log scale. In frequency domain it leads to the corner frequencies of the Lorentzians to be uniformly distributed on log scale [2,7]. *ii)* The number of traps in a given device is a random variable, assumed to be Poisson distributed. *iii)* The noise contribution A of a single trap is a random variable related to the trap impact on the drain current (or threshold voltage) and the trap occupancy, as discussed in detail in [1–4,7,15,20–22], among other works in the literature. In the work here presented no assumption is done regarding the statistical distribution of trap noise contribution A.

Since trap characteristic time constants are log-uniformly spread over several orders of magnitude, it is not adequate to use the total number of traps that may exist in a device as the modeling parameter. In our modeling work, trap density per frequency – or time – decade (N_{dec}) is used instead of the total number of traps [1–4]. Both parameters – N_{dec} and A – are employed in the frequency and time domain modeling of charge trapping produced noise. Hence, the model parameters in both frequency and time domain are the same: N_{dec} and A.

Experimentally, $N_{\rm dec}$ can be estimated from both the time and frequency domain data, provided the number of active traps in the observation window is determined. By increasing the time (or frequency) window, the number of observed (active) traps is expected to increase, while the other modeling parameter (A, the average amplitude of the trap contribution) is not expected to depend on the time (or frequency) window [1–4,7,15].

Thus, reporting solely the number of measured active traps is inadequate, as reporting the observation time window and sampling rate is critical for proper modeling of the RTN. Similarly, in frequency domain, when reporting number of traps observed, it is important to report the observation frequency window. Time and frequency windows are not related only to measurement duration, but also to parameters such as bandwidth, sampling rate or integration time, as discussed in this work.

In the next section it will be shown that the variance of the drain

E-mail address: gilson.wirth@ufrgs.br.

https://doi.org/10.1016/j.sse.2021.108140
Received 19 April 2021; Received in revised form 13 June 2021; Accepted 24 June 2021
Available online 27 June 2021
0038-1101/© 2021 Elsevier Ltd. All rights reserved.

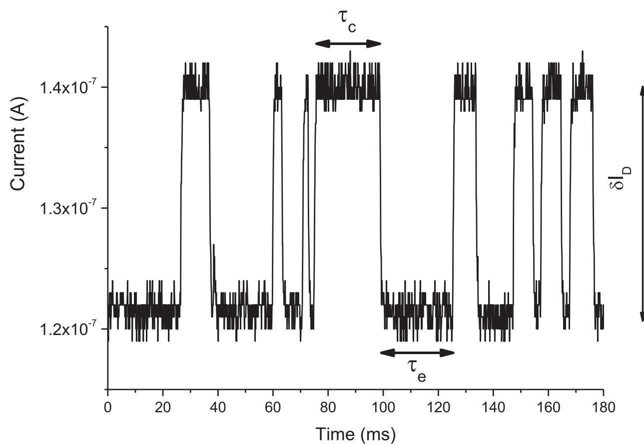

Fig. 1. Drain current variation over time, due to Random Telegraph Noise (RTN). If a single trap dominates noise behavior, trap occupancy switching leads to discrete fluctuations of amplitude δI_D, with τ_C and τ_E being the capture and emission time constants.

current (or threshold voltage) evaluated over a time window is expected to increase when the time window increases, similarly to the increase of integrated noise power when the integration frequency window increases. First, we discuss the case of a single trap, and then extend the discussion for the case of multiple traps. In section III we study the role of the observation window in detail, showing how changing its upper or lower boundaries affects the observed behavior. The observation window determines the number of traps that contribute to the observed stochastic fluctuations. In both sections II and III, the discussion is complemented by comparison of model equations to experimental data.

2. Electrical modeling of charge trapping

2.1. Single trap

In MOSFETs, switching traps randomly capture and emit charge carries from the channel region, causing the drain current I_D to randomly vary over time [1–15]. When a single trap is considered, I_D alternates between a high current state (when the trap is vacant) and a low current state (when the trap is occupied), as seen in Fig. 1. The average time in the high current state is τ_C, while τ_E is the average time in the low current state. The difference (fluctuation) in drain current between states is δI_D. The drain current fluctuations may be related to trap induced carrier number fluctuations and/or carrier mobility fluctuations [7,22]. Experimentally, RTN fluctuations are usually observed in the drain current, which can be translated into a threshold voltage fluctuations δV_T according to $\delta I_D = g_m \delta V_T$ [2,7,15]. The transconductance g_m may also be impacted, which may need to be considered. The conversion from drain current fluctuations to gate referred voltage fluctuations is discussed, e.g., in the chapter 1 of [22].

Since RTN is stationary, the statistical properties are independent of time t. If considering a time window, the statistical properties are independent of the origin (initial time t) of the window. However, due to the autocorrelation of RTN, the statistical properties depend on the size (duration, Δt) of the time window. This means that, for instance, if performing a measurement of I_D over time, the observed variance of I_D is expected to increase as measurement time progresses. Same applies to V_T, since the I_D fluctuations can be seen as V_T fluctuations.

First, we discuss the correlation of the RTN time series with itself at different time points, i.e., the autocorrelation. If considering a single trap, the autocorrelation (R_I) between values of the RTN at different times, as a function of the difference Δt between the two times (the time lag), is [16]:

$$R_I(\Delta t) = \delta I_D^2 \frac{\beta}{(\beta+1)^2} \exp\left(-\frac{\Delta t}{\tau}\right) \quad (1)$$

where $\beta = \tau_C/\tau_E$, with τ_C and τ_E being the capture and emission time constants, respectively. And $\frac{1}{\tau} = \frac{1}{\tau_c} + \frac{1}{\tau_E}$. Eq. (1) refers to the case where I_D fluctuations are considered. An equivalent equation may be written for the case where V_T fluctuations are considered, by replacing δI_D^2 with δV_T^2.

It is seen that at time lags much smaller than τ, the autocorrelation is maximum. As the time lag approaches τ the autocorrelation falls exponentially, and at a time lag much larger than τ the autocorrelation is minimum (negligible). This means that in a time window of duration much smaller than τ a negligible I_D (or V_T) variation is expected, while in a time window of duration much larger than τ a noticeable I_D variation is expected.

This is illustrated in Fig. 2. It shows the autocorrelation evaluated analytically, using Eq. (1), and numerically, from a measured I_D time series, which has 10,000 points of which 1800 points are shown in Fig. 1. The measured nMOSFET has a W/L equal to 800 nm/50 nm, gate bias was $V_{GS} = 1.6$ V and drain bias was $V_{DS} = 25$ mV. Sampling interval was 0.1 ms. The measurement spanned 1 s (10000 points were measured). Fabrication details are given in [17,18]. This device shows a clear two level RTN, indicating that the noise behavior is dominated by a single trap. The RTN amplitude δI_D is obtained from the histogram of the measured current amplitudes, with a double-Gaussian fitting, which reveals the two discrete current levels. After the two discrete current levels were determined, the measured time series was discretized to a RTN with only two current levels, and the capture and emission times evaluated. Parameter extraction methods are discussed, for instance, in [23–27]. For the RTN measured in this device δI_D is 18.5nA, τ_C is 10.7 ms and τ_E is 13.1 ms, which leads to τ equal to 5.89 ms. Note that for time lags much shorter than τ, it saturates at $\delta I_{Di}^2 \frac{\beta_i}{(\beta_i+1)^2} \stackrel{\text{def}}{=} A_{Ii}^2$, which for this particular trap is 8.5e-17 A^2.

It is seen that for time lags much shorter than τ, autocorrelation is maximum, meaning that a negligible I_D variation (fluctuation) is expected. As the time lag approaches τ, the autocorrelation sharply decreases. For time lags much longer than τ the autocorrelation is minimum, meaning that large I_D variations (fluctuation) are expected

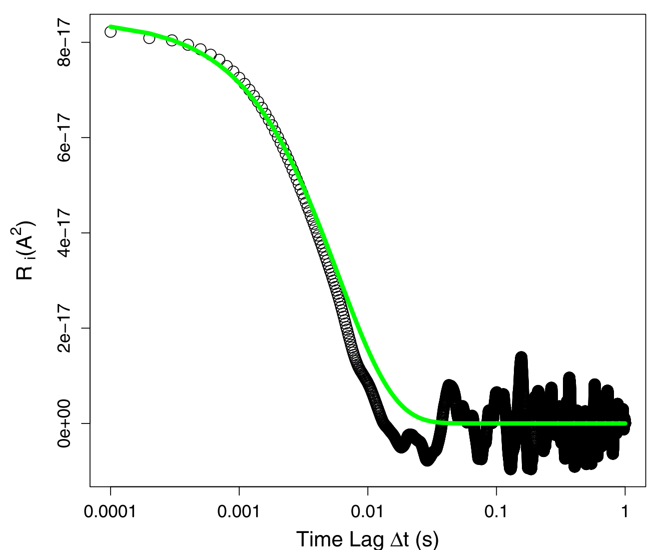

Fig. 2. Autocorrelation (R_I) of an RTN. The black circles are the numerical evaluation of the autocorrelation of the measured $I_D(t)$ time series. The green line is from the evaluation of the analytical Eq. (1). (For interpretation of the references to colour in this figure legend, the reader is referred to the web version of this article.)

for observations separated by these time lags.

The time domain behavior is related to the frequency domain behavior.

In frequency domain, the power spectral density (PSD) of the RTN produced by a single trap is [15,16]

$$S_I(f) = 4\delta I_D^2 \frac{\beta}{(\beta+1)^2}\frac{\tau}{1+(2\pi f\tau)^2} \tag{2}$$

As in the case of Eq. (1), an equivalent equation may be written for the case where the gate referred noise is considered, by replacing δI_D^2 with δV_T^2.

For a single trap, the noise power integrated over the circuit bandwidth of interest is given by the integration of (2) from f_L to f_H, which are the lower and upper boundaries of the bandwidth of interest [10]:

$$np_{BWi}(f_L, f_H) = \int_{f_L}^{f_H} S(f)df = \delta I_D^2 \frac{\beta}{(\beta+1)^2}\frac{2}{\pi}\left[\tan^{-1}\left(\frac{f_H}{f_i}\right) - \tan^{-1}\left(\frac{f_L}{f_i}\right)\right] \tag{3}$$

where $f_i = 1/(2\pi\tau)$.

Now we discuss the variance of the RTN time series, evaluated over a given observation interval Δt. The observation interval is called time window. It is

$$Var_i[\Delta I_{Di}(\Delta t)] = np_{BWi}(f_L, f_H) \tag{4}$$

where f_L is related to the duration – the maximum time (t_{max}) – of the time window, and f_H is related to the minimum time of the window (t_{min}) – usually the measurement time step, as discussed below. The index *i* is used because here we refer to the RTN generated by a single trap, the *i-th* trap, while in the next section we deal with multiple traps.

The noise power integrated over the bandwidth (np_{BWi}) is equivalent to the expected I_D variance, $Var_i[\Delta I_{Di}(\Delta t)]$ evaluated over the time interval Δt, with limits t_{min} and t_{max}. Note that $Var_i[\Delta I_{Di}(\Delta t)]$ is related to autocorrelation $R_I(\Delta t)$. However, it is not the same, since the autocorrelation captures the expected autocorrelation between points *separated by* Δt, while $Var_i[\Delta I_{Di}(\Delta t)]$ captures the variance *taken over all points in an interval* (time window) Δt.

Fig. 3 shows the variance of the measured I_D over time at different time windows (slices of the time series with different sizes). The analytical result from (4) is also shown. Data is from the same RTN for which the autocorrelation was shown in Fig. 2. The integrated noise power is evaluated analytically using Eqs. (3) and (4), with parameters δI_D, τ_C and τ_E as reported above. Note that for time intervals Δt much longer than τ, it goes to the limit value of $\delta I_{Di}^2 \frac{\beta_i}{(\beta_i+1)^2} = A_{Ii}^2$, where the amplitude contribution $A_{Ii}{}^2$ of the *ith* trap to the variance of I_D is the same as its contribution to low-frequency noise [1,2]. This is similar to the Lorentzian seen in frequency domain, which at low frequencies saturates (shows a plateau) which is proportional to A_{Ii}^2. The time and frequency windows (bandwidth) are related, as discussed in detail below.

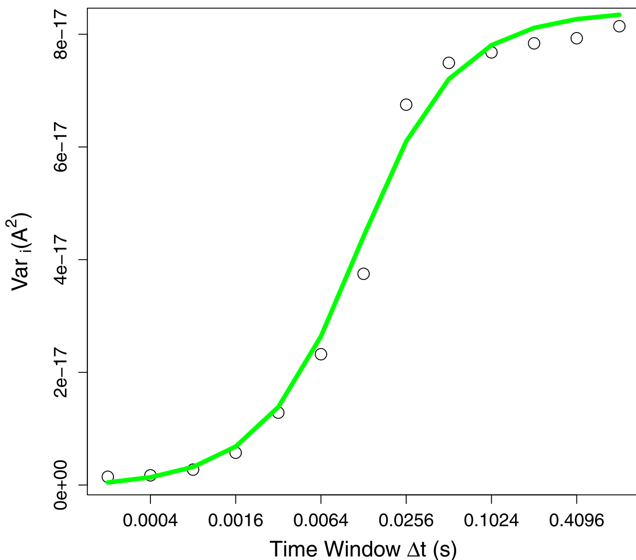

Fig. 3. Variance of the drain current I_D taken over time. The black circles are the numerical evaluation of the variance of the measured $I_D(t)$ time series. The green line is the result from the analytical Eq. (4). (For interpretation of the references to colour in this figure legend, the reader is referred to the web version of this article.)

2.2. Multiple traps

The value of the I_D deviation due to all active traps, here called ΔI_D, is then the sum of the contribution of all N_{trTW} traps found in a device and that are active in the time window. Assuming that the different traps are not correlated, the variance of the drain current evaluated over time is [1]

$$Var[\Delta I_D] = \sum_{i=1}^{N_{trTW}} Var_i[\Delta I_{Di}] \tag{5}$$

Due to the stochastic trap activity, the drain current may be different at each time instant. This drain current variability over time may be interpreted as a drain current jitter. The expected variance of the drain current taken over a time window is related to the time constants of the fastest and slowest trap that are active in the time window. These time constants are here called $t_{min,eff}$ and $t_{max,eff}$, respectively, and discussed in detail below. The expected variance of the drain current taken over time is evaluated as [1]

$$Var[\Delta I_D(t_{min,eff}, t_{max,eff})] = E[A_{Ii}{}^2]E[N_{trTW}] \tag{6}$$

where $E[N_{trTW}]$ is the expected (mean) number of traps per device active in the time window, and $E[A_{Ii}^2]$ is the expected (mean) noise contribution of a trap [1,2]. Here too an equivalent equation may be written for the case where V_T fluctuations are considered, by replacing A_{Ii}^2 with A_{Vi}^2 [1].

The number of traps expected to be active in the time window is [1]

$$E[N_{trTW}] = N_{dec}WL\log\left(\frac{t_{max,eff}}{t_{min,eff}}\right) \tag{7}$$

where N_{dec} is the trap density per unit area and time decade [1]. *W* and *L* are device width and length, respectively. $t_{min,eff}$ and $t_{max,eff}$ are the time constants of the fastest and slowest trap that are active in the time window of interest, respectively. The subscript *eff* is used to emphasize that we refer to the observable traps in the time window of interest, and not to all traps that may exist in the device. The time constant $t_{min,eff}$ of the fastest observable trap may be limited by the bandwidth of the measurement equipment, sampling time or integration time. The time constant $t_{max,eff}$ of the slowest observable trap is typically limited by the measurement duration.

$Var[\Delta I_D(t_{min,eff}, t_{max,eff})]$ is related to $np_{BW}(f_L, f_H)$, the expected noise power integrated over a frequency bandwidth (frequency window delimited by frequencies f_H and f_L). $Var[\Delta I_D(t_{min,eff}, t_{max,eff})]$ is proportional to the expected (average) number of traps active in the time window, and $np_{BW}(f_L, f_H)$is proportional to the expected (average) number of traps in the frequency window. From (8) in [2] and (13) in [1]:

$$np_{BW}(f_L, f_H) = \int_{f_L}^{f_H} S(f)df = E[A_i{}^2]N_{dec}WL\log\left(\frac{f_H}{f_L}\right)$$

Writing

$$E[Ntr_{BW}] = N_{dec}WL\log\left(\frac{f_H}{f_L}\right)$$

Leads to

$$np_{BW}(f_L, f_H) = E[A_i^2]E[Ntr_{BW}] \quad (8)$$

where f_H and f_L are the lower and upper boundaries of the frequency window (bandwidth). $Var[\Delta I_D(t_{min,eff}, t_{max,eff})]$ increases as the time window increases, while $np_{BW}(f_L, f_H)$ increases as the frequency window increases. In the next section, the role of the observation window is discussed in detail.

3. Observation window

In frequency domain, the size of the observation window depends on both f_H and f_L. These frequencies are not the frequencies of the fastest and slowest trap present in the device, but of the fastest and slowest observable ones. For instance, these frequencies may be set by the measurement instrumentation or by the bandwidth of the circuit, or by the choice of the integration limits. In time domain, the size of the time window depends on both $t_{min,eff}$ and $t_{max,eff}$. These time constants are not the time constants of the fastest and slowest trap present in the device, but of the fastest and slowest observable ones. If performing RTN electrical characterization, sampling time must be much shorter than the time constant (τ) of the fastest trap to be analyzed, and a large number of transitions (trap state switching events) needs to be measured, demanding a measurement time much larger than the τ of the slowest trap to be analyzed [12,13]. In frequency domain, to properly characterize the Lorentzian PSD due to a trap, the measurement bandwidth must also be adequate: f_L must be much lower than f_i, and f_H must be much higher than f_i. Hence, the observation window determines the number of observable traps, in both time and frequency domain.

Please note that since RTN is stationary, the result does not depend on the starting time of the time window, but only on its size. When performing a measurement, the observed variance does not depend on the clock time of measurement start, but it depends on the duration of the measurement. It is usually assumed that the time window starts at the first measured point. But any point of the measurement time series can be used as the starting point of the time window. In the results reported and discussed here, this feature was explored. When analyzing a time window that is smaller than the measured time series, the result presented is the average of the number of windows that fit in the measured time series. For instance, if the time series is twice the window of interest, two windows can be accommodated in the time series, the first covering the first half of the time series, and the second covering the other half. If the time series is 10 times the window of interest, ten windows can be accommodated in the time series, the first covering the first tenth of the time series, the second covering the second tenth, and so on. When evaluating the variance, this may be seen as a moving variance, where the time window moves over the available time series. Besides helping to confirm behavior, it also helps reducing statistical uncertainty. Similar approach can be used in frequency domain, where different windows of same size (same number of frequency decades) can be integrated, spanning the whole available frequency range.

In time domain, the slowest and fastest observable traps depend on the time window boundaries, $t_{min,eff}$ and $t_{max,eff}$, which are usually related to the total measurement time and sampling rate. First, we vary the time window by changing the total measurement time while keeping the sampling rate constant.

Fig. 4 shows experimental results for the variance of the drain current as a function of the time window ($t_{max,eff}/t_{min,eff}$), where the x-axis is in log scale. The measured nMOSFET has a W/L equal to 6 μm/50 nm, gate bias was $V_{GS} = 1.1$ V and drain bias was $V_{DS} = 25$ mV. Fabrication details are given in [17,18]. For this device, no clear RTN levels or discrete current jumps are visible. In the time domain measurement, the sampling interval was 1 ms, which is assumed to be $t_{min,eff}$. The measurement spanned approx. 10 s (about 10,000 points were measured). Hence, the length of the time window, $t_{max,eff}$ could be varied by choosing the number of subsequent measurement time points used to

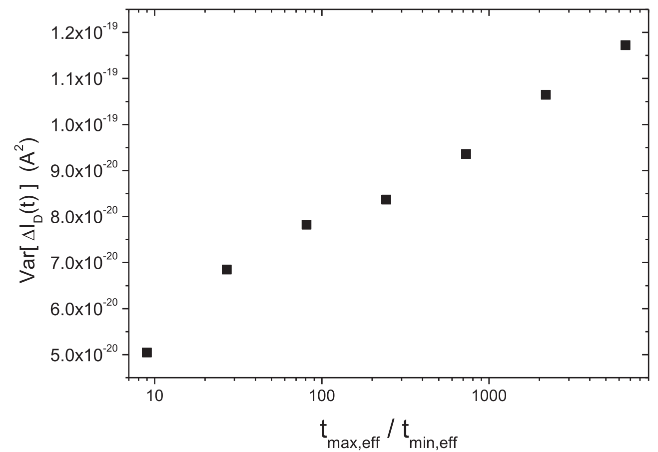

Fig. 4. Measured variance of the drain current fluctuation Var[$\Delta I_D(t)$] *versus* ($t_{max,eff}/t_{min,eff}$). The variance is seen to increase almost linearly with log($t_{max,eff}/t_{min,eff}$), as predicted by the model.

evaluate the variance. In other words, the observation window could be varied by varying $t_{max,eff}$, while $t_{min,eff}$ is constant. It is seen that the variance of drain current increases almost logarithmically with the time window, as modeled by Eqs. (6) and (7) above. Please note that the results shown in Fig. 4 also correspond well to the experimental data from other groups, as for instance the results reported in Figs. 7 and 12 of [5].

Fig. 5 shows the RTN times series measured on the same device for which the variance is reported in Fig. 4. Besides the measured time series, it also shows an envelope proportional to four times the standard deviation measured over the time window. From the figure we can see that the standard deviation of the RTN over a time window is dependent on the size of the window, increasing as the time window increases, as predicted by the model equations. The greater the observed time interval, the greater the expected I_D variation (for larger time windows, larger I_D fluctuations are expected). This is similar to the behavior reported for $1/f$ noise [2]. In the context of $1/f$, this is due to the fact that traps with frequencies below the measurement frequency window are filtered out. In the context of RTN, this is explained by the fact that traps slower than the measurement window will hardly change its state during

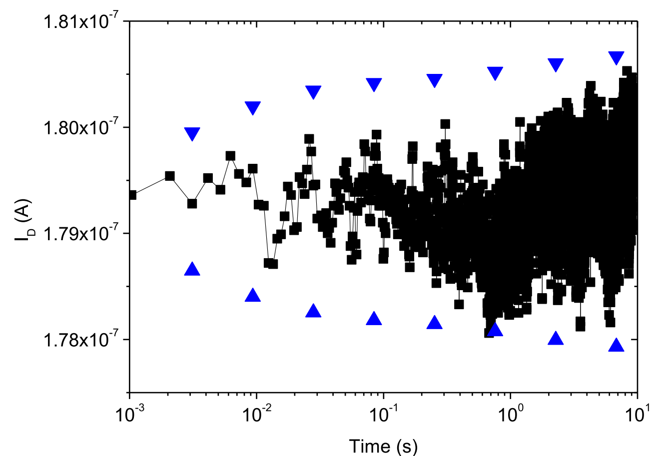

Fig. 5. The increase of the I_D fluctuations with time window. The black squares and line show the experimental data. The blue triangles show an envelope equal ± four times the standard deviation, evaluated from the measured time series. The standard deviation of RTN depends on the size of the observation window as predicted by the analytical model. (For interpretation of the references to colour in this figure legend, the reader is referred to the web version of this article.)

the observation. Referring to Fig. 3, this corresponds to the situation of short time scales in the x-axis, where the I_D variance due to the trap is negligible. But as time goes by, more traps are expected to become active and switch state.

The results shown in Fig. 5 also correspond well to the experimental RTN results reported by other groups, as for instance in Figs. 2 and 5 of [5], and Fig. 10 of [6]. The authors in [5,6] characterized this behavior using the concept of envelope, where the envelope is the difference between the maximum and minimum values found in the time window. However, this concept of envelope, when used to characterize RTN, may also capture a statistical bias that may exist by considering different number of measured data points [19]. As more measurements are considered in larger windows, the probability to find a large fluctuation is increased. Instead of using an envelope defined by the extreme values observed, the envelope may be assumed to be proportional to the standard deviation of RTN, as here proposed. By evaluating the variance over the time window, as done in this work, the RTN can be characterized without this statistical bias.

The time window can also be varied by changing the sampling interval (the time interval between successive measurements), related to $t_{min,eff}$, while keeping the measurement time, related to $t_{max,eff}$, fixed. For traps that are faster than the sampling rate of the measurement, switching events will be missed; if a trap switches faster than the integration time of the measurement equipment, an average value will be measured, and not the discrete values related to the different trap states. Hence, if the sampling interval is decreased, and the integration time is decreased accordingly as usually done in the experiments, the size of the time window is changed. Sampling interval is the inverse of sampling rate. Increasing sampling rate while keeping the measured time interval constant increases the time window ($t_{\max,\mathrm{eff}}/t_{\min,\mathrm{eff}}$), by decreasing $t_{\min,\mathrm{eff}}$. It may increase the number of traps that are observed to switch state. This can be obtained, for instance, measuring the device over a fixed time using different sampling rates, e.g., as done experimentally in the literature in [5,6]. If measurement time is kept fixed and sampling rate is increased, a larger number of points is measured, corresponding to a larger time window. In this case, the time window – and number of measured data points – is increased by decreasing the time interval between successive measurements. See, for instance, the behavior seen in Fig. 6 of [5]. To illustrate this behavior, we run Monte Carlo simulations, and show the results in Fig. 6, together with the analytical model results. In evaluating the analytical values and running Monte Carlo simulations, sampling rate range like the one reported for Fig. 6 of [5] is used. Again, our analytical model corresponds well to the experimental results reported in [5,6]. The Monte Carlo simulations were run using the methodology described in [1], which assumes that charge trapping and de-trapping are stochastic events governed by characteristic time constants which are uniformly distributed on a log scale, and that the average amplitude contribution of a trap (A) does not depended on the time window (does not depend on sampling rate). After running the Monte Carlo simulations, the standard deviation of the simulated time window is evaluated. The envelope is assumed to be proportional to the evaluated standard deviation. The analytical results are obtained from (6) assuming that $E[A_{Ii}{}^2]$ does not depend on the time window and that $E[N_{trTW}]$ is related to the time window as given by (7).

4. Conclusions

The dependence of the RTN statistical parameters on the observation window was studied by analytical modeling and analysis of experimental results. First, the noise produced by a single trap is discussed, starting by the study of its autocorrelation. Then, the noise generated by multiple traps is studied. Increasing the observation window increases the number of observable traps. The size of the observation window was varied, by changing its upper and lower boundaries, and the observed behavior discussed in detail, relating it to trap density. This discussion was illustrated by presenting experimental results. The discussions done here help to better interpret and present experimental results.

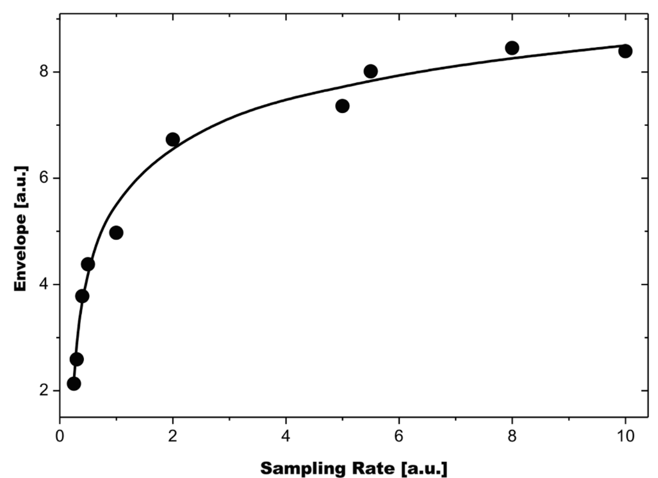

Fig. 6. The impact of sampling rate on an envelope considered to be proportional to the expected standard deviation of I_D. Line shows analytical model results, while circles show Monte Carlo simulation results. Results are obtained by assuming that the sampling rate changes while measurement time is kept fixed: the time window is varied by changing $t_{\min,\mathrm{eff}}$ while keeping $t_{max,eff}$ fixed.

Declaration of Competing Interest

The authors declare that they have no known competing financial interests or personal relationships that could have appeared to influence the work reported in this paper.

References

[1] Wirth G. Time-dependent random threshold voltage variation due to random telegraph noise. IEEE Trans Electron Dev 2021;68(1):17–23. https://doi.org/10.1109/TED.2020.3039204.

[2] Wirth GI, da Silva R, Brederlow R. Statistical model for the circuit bandwidth dependence of low-frequency noise in deep-submicrometer MOSFETs. IEEE Trans Electron Devices 2007;54(2):340–5. https://doi.org/10.1109/TED.2006.888672.

[3] Banaszeski da Silva M, Tuinhout HP, Zegers-van Duijnhoven A, Wirth GI, Scholten AJ, A Physics-Based Statistical RTN Model for the Low Frequency Noise in MOSFETs. In: IEEE Transactions on Electron Devices, vol. 63, no. 9, pp. 3683–3692, 2016, doi: 10.1109/TED.2016.2593916.

[4] Both TH, Croon JA, Banaszeski da Silva M, Tuinhout HP, Scholten AJ, Zegers-van Duijnhoven A, et al. Autocorrelation analysis as a technique to study physical mechanisms of MOSFET low-frequency noise. IEEE Trans Electron Devices 2017;64 (7):2919–26. https://doi.org/10.1109/TED.2017.2703671.

[5] Mehedi M, Tok KH, Zhang JF, Ji Z, Ye Z, Zhang W, et al. An assessment of the statistical distribution of random telegraph noise time constants. IEEE Access 2020; 8:182273–82. https://doi.org/10.1109/Access.628763910.1109/ACCESS.2020.3028747.

[6] Duan M, et al., Key issues and techniques for characterizing time-dependent device-to-device variation of SRAM. In: 2013 IEEE International Electron Devices Meeting, Washington, DC, 2013, pp. 31.3.1-31.3.4, doi: 10.1109/IEDM.2013.6724730.

[7] Grasser T, editor. Noise in Nanoscale Semiconductor Devices. Springer; 2020. ISBN 978-3-030-37500-3.

[8] Ioannidis EG, Rohracher K, Enichlmair H. State-of-the-art low frequency noise performance of n-MOSFET for analog/RF applications. Solid-State Electron 2020; 167:107754. https://doi.org/10.1016/j.sse.2019.107754.

[9] Mavredakis N, Pflanzl W, Seebacher E, Bucher M. Methodology for 1/f noise parameter extraction for high-voltage MOSFETs. Solid-State Electron 2015;103: 202–8. https://doi.org/10.1016/j.sse.2014.07.011.

[10] da Silva R, Wirth GI, Brederlow R. Novel analytical and numerical approach to modeling low-frequency noise in semiconductor devices. Phys A 2006;362(2): 277–88. https://doi.org/10.1016/j.physa:2005.11.014.

[11] Cretu B, Boudier D, Simoen E, Veloso A, Collaert N, Claeys C. Improved physics-based analysis to discriminate the flicker noise origin at very low temperature and drain voltage polarization. Solid-State Electron 2020;171:107771. https://doi.org/10.1016/j.sse.2020.107771.

[12] Puglisi FM, Pavan P. Guidelines for a reliable analysis of random telegraph noise in electronic devices. IEEE Trans Instrum Meas 2016;65(6):1435–42. https://doi.org/10.1109/TIM.2016.2518880.

[13] Shamsur Rouf, Zeynep Çelik-Butler ASM. Channel hot carrier induced volatile oxide traps responsible for random telegraph signals in submicron pMOSFETs, Solid-State Electronics, v. 164, 2020, 107745, doi: 10.1016/j.sse.2019.107745.
[14] Pirro L, Ionica I, Cristoloveanu S, Ghibaudo G. Low-frequency noise in bare SOI wafers: experiments and model. Solid-State Electron 2016;125:167–74. https://doi.org/10.1016/j.sse.2016.07.012.
[15] Kirton MJ, Uren MJ. Noise in solid-state microstructures: a new perspective on individual defects, interface states and low-frequency (1/ƒ) noise. Adv Phys 1989; 38(4):367–468. https://doi.org/10.1080/00018738900101122.
[16] Machlup S. Noise in semiconductors: spectrum of a two-parameter random signal. J Appl Phys 1954;25(3):341–3. https://doi.org/10.1063/1.1721637.
[17] Horstmann JT, Hilleringmann U, Goser KF. Matching analysis of deposition defined 50-nm MOSFET's. IEEE Trans Electron Devices 1998;45(1):299–306. https://doi.org/10.1109/16.658845.
[18] Wirth G, Hilleringmann U, Horstmann JT, Goser K. Mesoscopic transport phenomena in ultrashort channel MOSFETs. Solid-State Electron 1999;43(7): 1245–50. https://doi.org/10.1016/S0038-1101(99)00060-X.
[19] Wirth G, Both T, Silva MB. Towards Unifying the Statistical Modeling of Charge Trapping in Time and Frequency Domain. 2021 IEEE Latin America Electron Dev. Conf. (LAEDC), pp. 1-3, doi: 10.1109/LAEDC51812.2021.9437944.
[20] Grasser T, Rott K, Reisinger H, Waltl M, Franco J, Kaczer B. A unified perspective of RTN and BTI, 2014 IEEE International Reliability Physics Symposium, 2014, pp. 4A.5.1-4A.5.7, doi: 10.1109/IRPS.2014.6860643.
[21] Kaczer B, Roussel PJ, Grasser T, Groeseneken G. Statistics of multiple trapped charges in the gate oxide of deeply scaled MOSFET devices—application to NBTI. IEEE Electron Device Lett 2010;31(5):411–3. https://doi.org/10.1109/LED.2010.2044014.
[22] Grasser T, editor. Bias Temperature Instability for Devices and Circuits. New York, NY: Springer New York; 2014.
[23] Yuzhelevski Y, Yuzhelevski M, Jung G. Random telegraph noise analysis in time domain. Rev Sci Instrum 2000;71(4):1681–8. https://doi.org/10.1063/1.1150519.
[24] Nagumo T, Takeuchi K, Yokogawa S, Imai K, Hayashi Y. New Analysis Methods for Comprehensive Understanding of Random Telegraph Noise. 2009 IEEE International Electron Devices Meeting (IEDM), Dec. 2009, pp. 1–4. doi: 10.1109/iedm.2009.5424230.3.
[25] Martin-Martinez J, Diaz J, Rodriguez R, Nafria M, Aymerich X. New weighted time lag method for the analysis of random telegraph signals. IEEE Electron Device Lett 2014;35(4):479–81. https://doi.org/10.1109/LED.2014.2304673.
[26] Puglisi FM, Pavan P. RTN analysis with FHMM as a tool for multi-trap characterization in HfOX RRAM. In: IEEE International Conference of Electron Devices and Solid-state Circuits; 2013. p. 1–2. 10.1109/EDSSC.2013.6628059.
[27] Frank DJ, Miki H. Analysis of oxide traps in nanoscale MOSFETs using random telegraph noise. In: Grasser T, editor. Bias temperature instability for devices and circuits. New York, NY: Springer New York; 2014. p. 111–34. https://doi.org/10.1007/978-1-4614-7909-3_5.

Gilson Wirth received the B.S.E.E and M.Sc. degrees from the Universidade Federal do Rio Grande do Sul, Brazil, in 1990 and 1994, respectively. In 1999 he received the Dr.-Ing. degree in Electrical Engineering from the University of Dortmund, Dortmund, Germany. He is currently a professor at the Electrical Eng. Depart. at Univ. Federal do Rio Grande do Sul – UFRGS (since January 2007). From July 2002 to December 2006 he was professor and head of the Computer Engineering Department, Univ. Estadual do Rio Grande do Sul – UERGS. His current research work focuses on modeling and electrical stimulation of charge trapping in the context of Bias Temperature Instability (BTI), Low-Frequency Noise (1/f and RTN) and Hot Carrier Injection (HCI). He has also worked on ionizing radiation effects (TID and SET/SEU) on semiconductor devices. He focuses on collaborative work with academia and industry. He has stablished successful collaborative work with different companies and research groups in Europe, North and South America, and China. He is currently a Distinguished Lecturer of the IEEE Electron Devices Society. He also was a distinguished lecturer of the IEEE Circuits and Systems Society (term 20102011). An updated list of publications may be found at http://lattes.cnpq.br/1745194055679908 or https://publons.com/researcher/3063393/gilson-wirth/.